

The Highly Unsaturated Binuclear Chromium Carbonyl $\text{Cr}_2(\text{CO})_8$

Se Li, R. Bruce King, and Henry F. Schaefer, III*

Department of Chemistry and Center for Computational Chemistry, University of Georgia, Athens, Georgia 30602

Received: February 16, 2004; In Final Form: May 27, 2004

The first structural characterization of the highly unsaturated dichromium carbonyl $\text{Cr}_2(\text{CO})_8$ is reported using density functional theory (DFT). $\text{Cr}_2(\text{CO})_8$ is predicted to have a short metal–metal bond length of 2.30 Å (B3LYP) or 2.28 Å (BP86). The minimum-energy structure exhibits distorted C_s symmetry, with nonequivalent chromium atoms and two equivalent asymmetrically bridging carbonyls. A high-symmetry (D_{2d}) structure with a nominal chromium–chromium quadruple bond lies ~ 22 kcal/mol higher in energy. Three other higher-energy structures are also found, including two geometries with two bridging carbonyls best interpreted as four-electron donors. The dissociation energy of $\text{Cr}_2(\text{CO})_8$ to the fragments $2\text{Cr}(\text{CO})_4$ or $\text{Cr}(\text{CO})_3$ plus $\text{Cr}(\text{CO})_5$ is predicted to be about 34 kcal/mol (B3LYP) or 44 kcal/mol (BP86), indicating that $\text{Cr}_2(\text{CO})_8$, like $\text{Cr}_2(\text{CO})_9$ but unlike $\text{Cr}_2(\text{CO})_{10}$ and $\text{Cr}_2(\text{CO})_{11}$, is stable with respect to dissociation into its fragments.

1. Introduction

In recent years, there have been several studies of highly unsaturated homoleptic binuclear carbonyls of the first-row transition metals. This work has included the carbonyls $\text{Co}_2(\text{CO})_5$,¹ $\text{Fe}_2(\text{CO})_6$,² and $\text{Mn}_2(\text{CO})_7$,³ all of which are required by the simple 18-electron rule⁴ to have formal metal–metal quadruple bonds,⁵ assuming that all of their carbonyl groups are simple two-electron donors. Indeed, in all three cases, structures were found with short metal–metal distances [2.171 Å for $\text{Co}_2(\text{CO})_5$, 2.00 Å for $\text{Fe}_2(\text{CO})_6$, and 2.21–2.26 Å for $\text{Mn}_2(\text{CO})_7$], consistent with such metal–metal quadruple bonding. However, for $\text{Fe}_2(\text{CO})_6$ and $\text{Mn}_2(\text{CO})_7$, other structures were also found having longer metal–metal bond distances and two bridging CO groups oriented to suggest four-electron rather than the usual two-electron donors. In these cases, the 18-electron rule would require formal metal–metal double bonding rather than formal metal–metal quadruple bonding, in accord with the lengthened metal–metal bond distances found computationally.

The system of homoleptic binuclear carbonyls of chromium is different from those of manganese, iron, and cobalt in a number of significant ways. Most obvious to the experimentalist is the fact that, among the species predicted by the 18-electron rule to have formal metal–metal single bonds, the molecule $\text{Cr}_2(\text{CO})_{11}$ ⁶ is not isolable in contrast to $\text{Mn}_2(\text{CO})_{10}$, $\text{Fe}_2(\text{CO})_9$, and $\text{Co}_2(\text{CO})_8$, which are all stable metal carbonyls and even commercially available. Consistent with this experimental observation are our studies of $\text{Cr}_2(\text{CO})_{11}$ indicating a relatively long chromium–chromium distance (no B3LYP value is available, 3.15 Å by BP86) and thermodynamic instability with respect to $\text{Cr}(\text{CO})_6$ and $\text{Cr}(\text{CO})_5$. A similar thermodynamic instability was predicted for $\text{Cr}_2(\text{CO})_{10}$.⁷ Only in the case of the more highly unsaturated $\text{Cr}_2(\text{CO})_9$ ⁸ was a thermodynamically stable binuclear derivative found with a short chromium–chromium distance [2.315 Å (B3LYP) or 2.285 Å (BP86)] consistent with the $\text{Cr}\equiv\text{Cr}$ triple bond required by the 18-electron rule.

The objective of the present study was to extend this computational work on homoleptic binuclear chromium carbonyls to the next most highly unsaturated member, namely, $\text{Cr}_2(\text{CO})_8$, required by the 18-electron rule to contain a chromium–chromium quadruple bond. Such chromium–chromium quadruple bonds have been postulated for chromium(II) compounds with short chromium–chromium distances including chromium(II) acetate, $\text{Cr}_2(\text{O}_2\text{CCH}_3)_4\cdot 2\text{H}_2\text{O}$ (2.362 Å),⁹ which has been known since the 19th century, as well as more recently discovered strictly organometallic derivatives exhibiting much shorter chromium–chromium distances such as $\text{Li}_4[\text{Cr}_2(\text{CH}_3)_8]\cdot 4\text{C}_4\text{H}_8\text{O}$ (1.98 Å),¹⁰ $\text{Cr}_2(\eta^3\text{-C}_3\text{H}_5)_4$ (1.98 Å),¹¹ and the ultra-short $\text{Cr}_2(\text{DMP})_4$ (1.85 Å).^{12,13} However, no binuclear chromium(0) compound is known with a short chromium–chromium distance and an electronic configuration suggestive of quadruple bonding.

2. Theoretical Methods

Our basis set for C and O begins with Dunning's standard double- ζ contraction¹⁴ of Huzinaga's primitive sets¹⁵ and is designated (9s5p/4s2p). The double- ζ plus polarization (DZP) basis set used here adds one set of pure spherical harmonic d functions with orbital exponents $\alpha_d(\text{C}) = 0.75$ and $\alpha_d(\text{O}) = 0.85$ to the DZ basis set. For Cr, our loosely contracted DZP basis set, the Wachters' primitive set,¹⁶ is used but is augmented by two sets of p functions and one set of d functions, contracted following Hood, Pitzer, and Schaefer,¹⁷ and designated (14s11p6d/10s8p3d). For $\text{Cr}_2(\text{CO})_8$, there are 338 contracted Gaussian functions in the present DZP basis set.

Electron correlation effects were included employing DFT methods that are acknowledged to be a practical and effective computational tool, especially for organometallic compounds.¹⁸ Among density functional procedures, the most reliable approximation is often thought to be the hybrid Hartree–Fock (HF)/DFT method B3LYP, which uses the combination of the three-parameter Becke exchange functional with the Lee–Yang–Parr correlation functional.^{19,20} However, another DFT method, which combines Becke's 1988 exchange functional with Perdew's 1986 nonlocal correlation functional method (BP86),

* Corresponding author. E-mail: hfs@uga.edu.

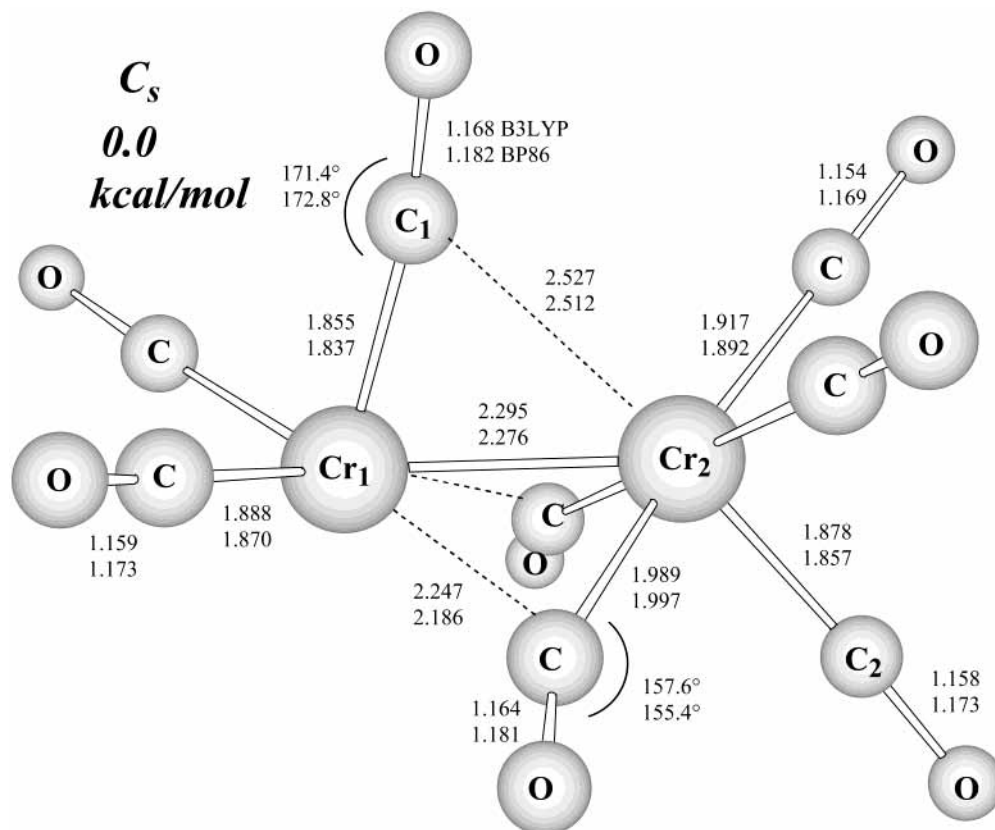


Figure 1. Asymmetrically dibridged global minimum-energy structure for singlet $\text{Cr}_2(\text{CO})_8$ with C_s symmetry. The plane of symmetry includes $\text{Cr}(1)$, $\text{Cr}(2)$, and the two carbonyl groups $\text{C}(1)\text{O}$ and $\text{C}(2)\text{O}$. This structure has one small imaginary harmonic vibrational frequency for BP86 and none with the B3LYP method. Distances are reported in angstroms.

TABLE 1: Relative Energies of Singlet $\text{Cr}_2(\text{CO})_8$ and Its Dissociation Limits $2\text{Cr}(\text{CO})_4$ and $\text{Cr}(\text{CO})_3 + \text{Cr}(\text{CO})_5$

species	symm	state	Cr–Cr bond distance (Å)		imaginary harmonic vibrational frequency		relative energy (kcal/mol)	
			B3LYP	BP86	B3LYP	BP86	B3LYP	BP86
$\text{Cr}_2(\text{CO})_8$	C_s	$^1A'$	2.295	2.276	none	28i (a'')	0.0	0.0
	C_i	1A	2.514	2.469	36i (a_u)	35i (a_u)	7.9	7.5
	C_{2v}	1A_1	2.747	2.712	53i (b_2)	65i (b_2)	13.4	18.7
	D_{2d}	1A_1	2.279	2.217	none	none	20.1	22.9
	C_s	1A_1	2.327	2.267	none	none	23.2	24.7
$2\text{Cr}(\text{CO})_4$	C_{2v}	1A_1			none	none	34.2	43.9
$\text{Cr}(\text{CO})_3 + \text{Cr}(\text{CO})_5$	C_{3v} and C_{4v}	1A_1 and 1A_1			none	none	34.5	44.0

has proven perhaps even more effective²¹ for organotransition metal systems and is also used in this research.^{22,23}

We fully optimized the geometries of all structures with the DZP B3LYP and DZP BP86 methods. At the same levels, we also computed the vibrational frequencies by evaluating analytically the second derivatives of the energy with respect to the nuclear coordinates. The corresponding infrared intensities were evaluated analytically as well. All of the computations were carried out with the Gaussian 94 program,²⁴ in which the fine grid (75 302) is the default for evaluating integrals numerically and the tight (10^{-8} hartree) designation is the default for the self-consistent field (SCF) convergence.

In the search for minima using all currently implemented DFT methods, low-magnitude imaginary vibrational frequencies are suspect because of significant limitations in the numerical integration procedures used in the DFT computations. Thus, for an imaginary vibrational frequency with a magnitude less than 100 cm^{-1} , there is an energy minimum identical or very close to the structure of the stationary point in question. Therefore, we generally do not follow such low imaginary vibrational

frequencies. In the present case, the B3LYP and BP86 methods agree with each other fairly well for predicting the structural characteristics of $\text{Cr}_2(\text{CO})_8$. Slight discrepancies in the appearance of possibly artifactual imaginary harmonic vibrational frequency remain, however.

3. Results and Discussion

3.1. Geometric Structures. Five isomers of $\text{Cr}_2(\text{CO})_8$ stoichiometry, bridged and unbridged, were found in this computational study (Table 1). The B3LYP and BP86 functionals agree in the relative energetic orders of these isomers.

The lowest-lying minimum for $\text{Cr}_2(\text{CO})_8$ has an unsymmetrical dibridged $(\text{OC})_3\text{CrCr}(\text{CO})_5$ structure with C_s symmetry (Figure 1), which can be derived directly from the C_s structure⁸ of unsaturated $\text{Cr}_2(\text{CO})_9$. Thus, removal of one terminal CO group from $\text{Cr}(1)$ in $\text{Cr}_2(\text{CO})_9$ leads to the lowest-lying structure of $\text{Cr}_2(\text{CO})_8$. In this structure, the chromium–chromium distance is 2.295 Å (B3LYP) or 2.276 Å (BP86), which is shortened slightly by 0.02 Å (B3LYP) or 0.01 Å (BP86) from the

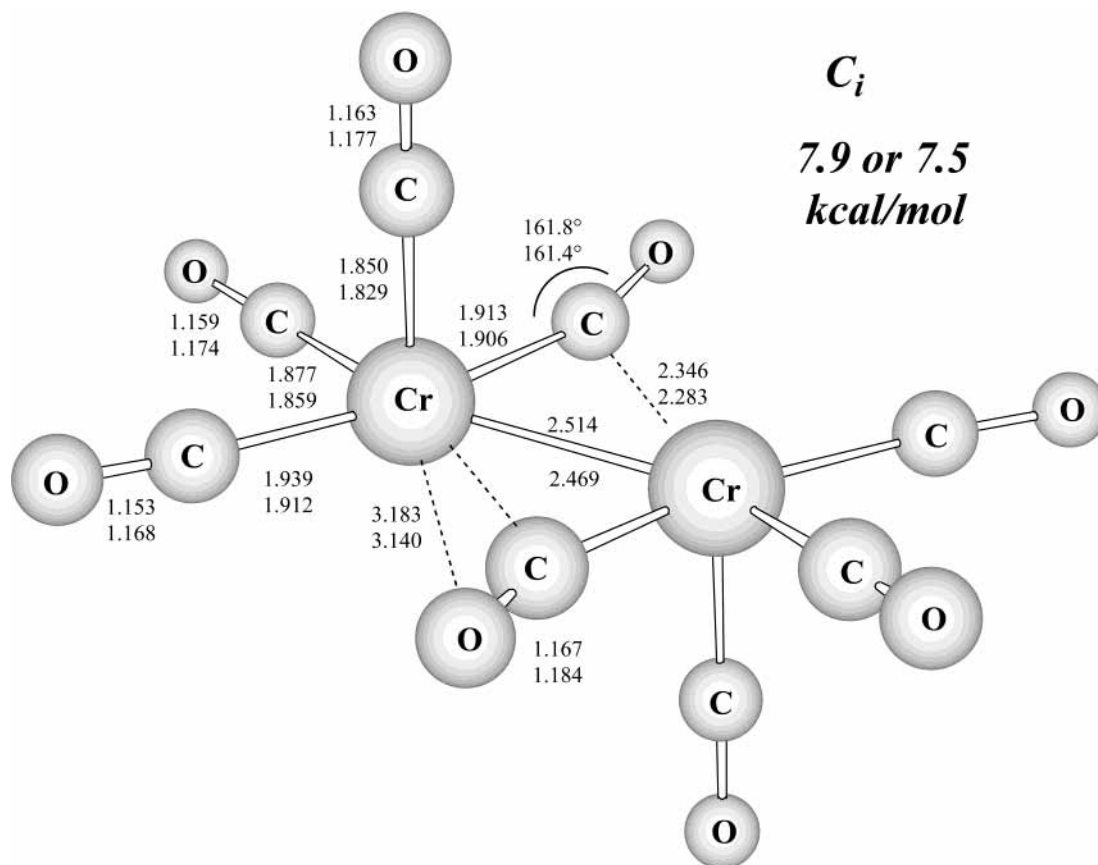


Figure 2. Symmetrically dibridged structure for singlet $\text{Cr}_2(\text{CO})_8$ with C_i symmetry. This structure has one small imaginary harmonic vibrational frequency with both the B3LYP and BP86 methods. Distances are reported in angstroms.

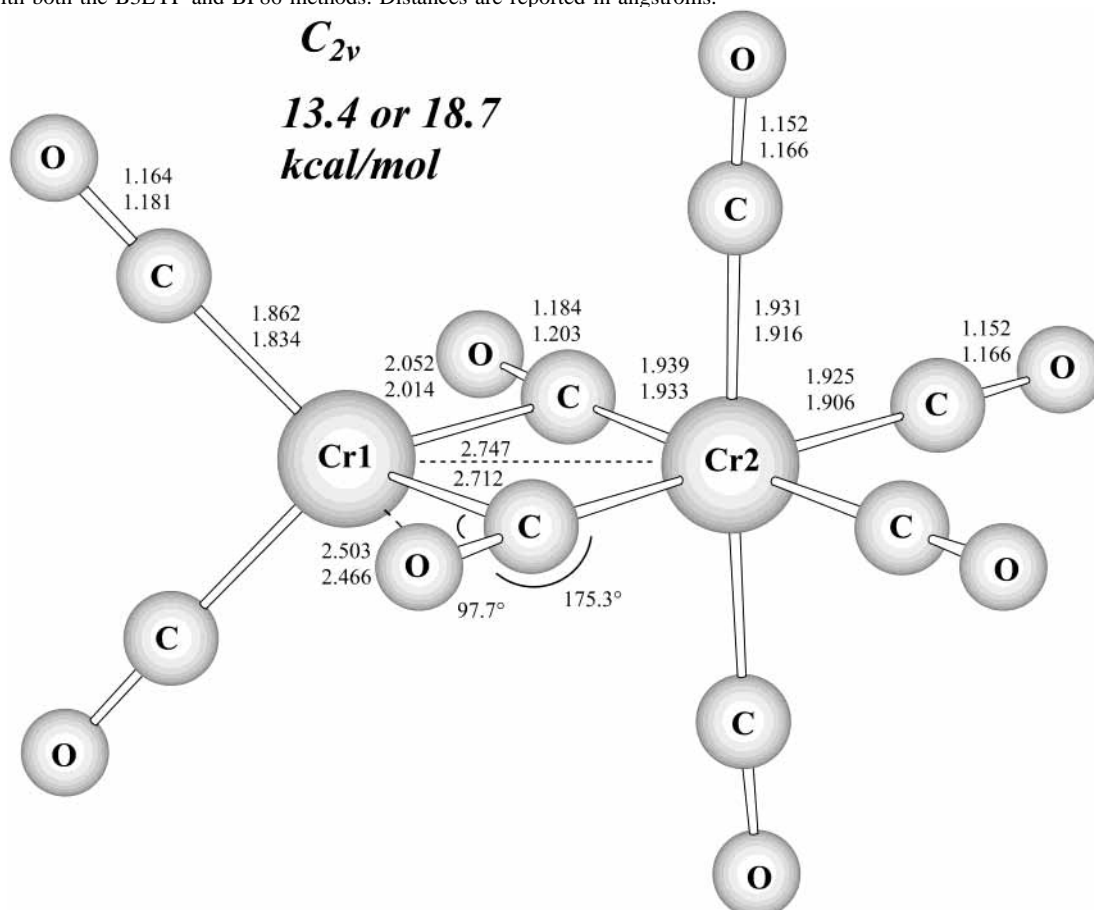


Figure 3. Asymmetrically dibridged structure for singlet $\text{Cr}_2(\text{CO})_8$ with C_{2v} symmetry. This structure has one small imaginary harmonic vibrational frequency with both the B3LYP and BP86 methods. Distances are reported in angstroms.

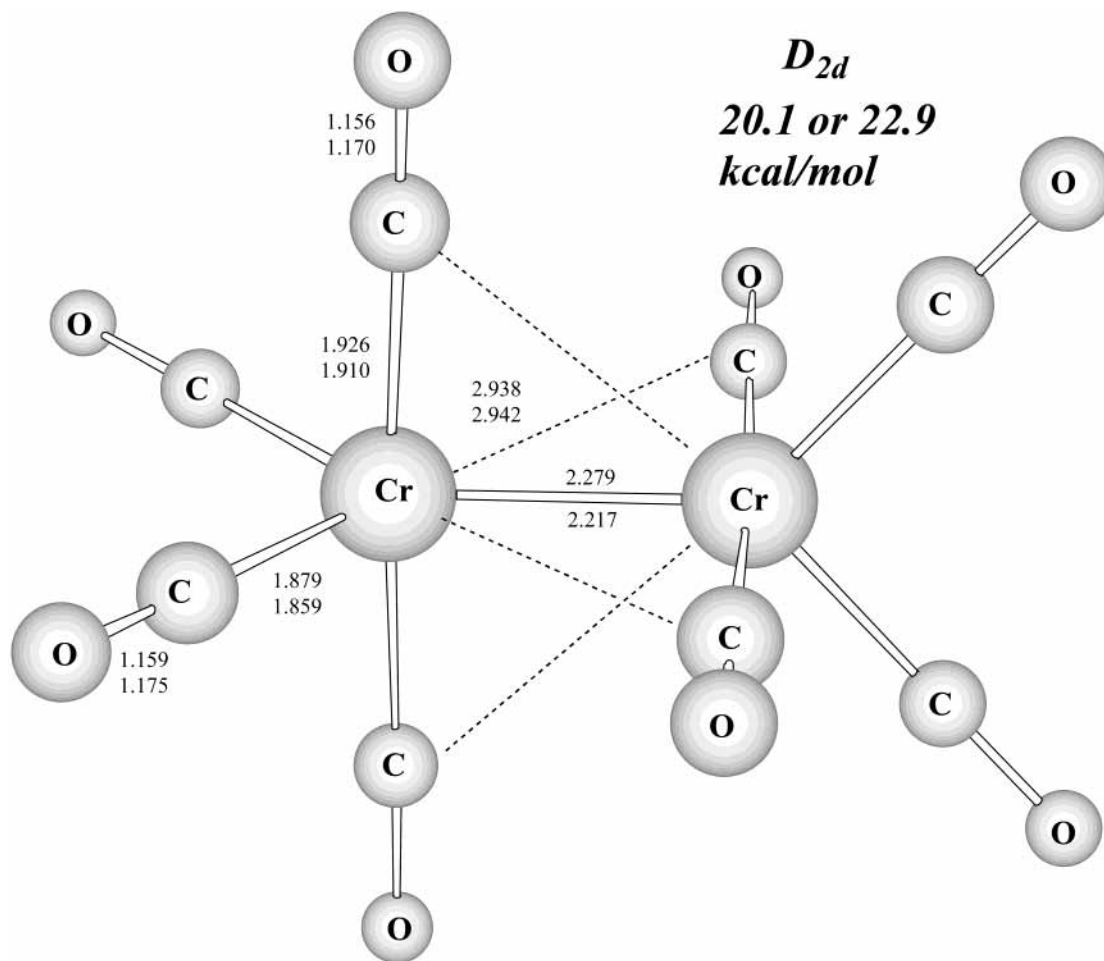


Figure 4. Symmetrically nonbridged minimum-energy structure for singlet $\text{Cr}_2(\text{CO})_8$ with D_{2d} symmetry. This structure has all real harmonic vibrational frequency with both the B3LYP and BP86 methods. Distances are reported in angstroms.

chromium–chromium distances computed for $\text{Cr}_2(\text{CO})_9$. In going from $\text{Cr}_2(\text{CO})_9$ to this $\text{Cr}_2(\text{CO})_8$ structure, one of the three bridging CO groups, which is a symmetrical bridge in $\text{Cr}_2(\text{CO})_9$, becomes a very unsymmetrical semibridging CO in $\text{Cr}_2(\text{CO})_8$ with Cr–C distances of 1.855 Å (B3LYP) or 1.837 Å (BP86) to Cr(1) and 2.527 Å (B3LYP) or 2.512 Å (BP86) to Cr(2). The approximate coordination geometries of the chromium atoms (Figure 1) are square pyramidal for Cr(1) and octahedral for Cr(2) if the ~ 2.5 Å distance from the semibridging CO group to Cr(2) is counted as a Cr–C bond. The bond angle Cr(1)CO relaxes from 163.9° (B3LYP) or 162.4° (BP86) in $\text{Cr}_2(\text{CO})_9$ to 171.4° (B3LYP) or 172.8° (BP86) in this structure of $\text{Cr}_2(\text{CO})_8$. Consequently, the Cr(1)–C(1) distance decreases from 1.934 Å (B3LYP) or 1.940 Å (BP86) in $\text{Cr}_2(\text{CO})_9$ to 1.855 Å (B3LYP) or 1.837 Å (BP86) in $\text{Cr}_2(\text{CO})_8$. These results are both suggestive of a stronger interaction between Cr(1) and C(1) in $\text{Cr}_2(\text{CO})_8$ relative to $\text{Cr}_2(\text{CO})_9$. Meanwhile, the interaction between Cr(2) and C(1) is weakened from $\text{Cr}_2(\text{CO})_9$ to $\text{Cr}_2(\text{CO})_8$, which leads to a longer Cr(2)–C(1) distance and a shorter Cr(2)–C(2) distance. Otherwise, the structures of this lowest-energy isomer of $\text{Cr}_2(\text{CO})_8$ and $\text{Cr}_2(\text{CO})_9$ are very similar. Thus, in both structures, the two chromium atoms have square-planar $\text{Cr}(\text{CO})_2(\mu\text{-CO})_2$ environments involving two bridging carbonyl groups and two terminal carbonyl groups. The B3LYP functional predicts all real vibrational frequencies. However, the BP86 functional computes a very small imaginary frequency (28 cm^{-1}).

The isomer of next lowest energy is a C_i symmetrical dibridged $(\text{OC})_4\text{CrCr}(\text{CO})_4$ structure lying about 8 kcal/mol

above the global minimum (Figure 2). The chromium–chromium bond distance in this structure is significantly longer than that for the global minimum [2.514 Å (B3LYP) or 2.469 Å (BP86)]. Notably, the two bridging carbonyls are coplanar with the two chromium atoms and bent to about 160°. Both B3LYP and BP86 functionals predict a very small imaginary frequency (36 and 35 cm^{-1} , respectively), which might be due to numerical noise.

The third $\text{Cr}_2(\text{CO})_8$ isomer also has a dibridged structure and lies energetically above the global minimum by 13.4–18.7 kcal/mol (Figure 3). Notably, this structure has a significantly longer chromium–chromium distance, namely, 2.747 Å (B3LYP) or 2.712 Å (BP86). For the two bridging COs, the Cr–C–O angles are roughly linear and the Cr–O distance is significantly shorter [2.503 Å (B3LYP) or 2.466 Å (BP86)] than in the other $\text{Cr}_2(\text{CO})_8$ isomers. This suggests a direct interaction between the chromium and oxygen atoms of these two bridging CO groups, in accord with these CO groups functioning as four-electron donors rather than the usual two-electron donors. In this case, the chromium–chromium bond needs only to be a double bond rather than a quadruple bond to give both chromium atoms the favored 18-electron configuration. This conclusion is in accord with the significantly longer chromium–chromium distance in this isomer as compared with the other isomers (Table 1). Both the B3LYP and BP86 functionals give consistent agreement for the vibrational frequency calculations leading to similar small imaginary frequencies (53 and 65 cm^{-1} , respectively).

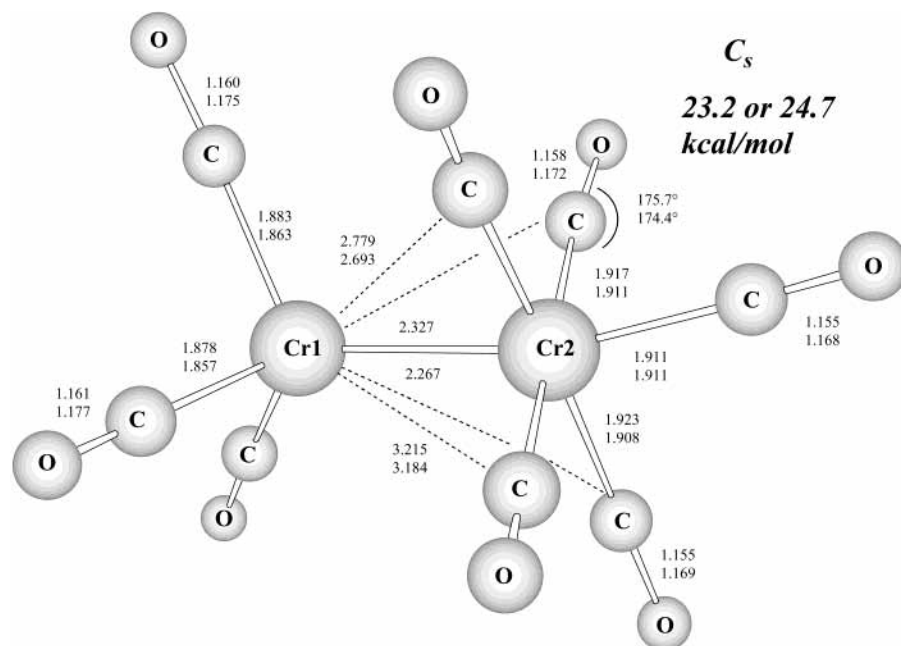


Figure 5. Asymmetrically nonbridged minimum-energy structure for singlet $\text{Cr}_2(\text{CO})_8$ with C_s symmetry. This structure has all real harmonic vibrational frequency with both the B3LYP and BP86 methods. Distances are reported in angstroms.

The energetically highest-lying isomers found for $\text{Cr}_2(\text{CO})_8$ are two nonbridged structures, namely, the symmetrical D_{2d} isomer $(\text{OC})_4\text{CrCr}(\text{CO})_4$ and the unsymmetrical C_s isomer $(\text{OC})_3\text{CrCr}(\text{CO})_5$ (Figures 4 and 5). These isomers lie approximately 20 kcal/mol above the global minimum and are predicted to be genuine minima by both the B3LYP and BP86 functionals. The D_{2d} structure contains the shortest chromium–chromium distance [2.279 Å (B3LYP) and 2.217 Å (BP86)] among the five isomers of $\text{Cr}_2(\text{CO})_8$. The unsymmetrical $(\text{OC})_3\text{CrCr}(\text{CO})_5$ structure of the C_s isomer is very similar to that of the unsymmetrical C_s isomer $(\text{OC})_3\text{MnMn}(\text{CO})_5$ of $\text{Mn}_2(\text{CO})_8$, lying only ~ 2 kcal/mol above the more symmetrical D_{2d} global minimum of $\text{Mn}_2(\text{CO})_8$.^{3,25} The chromium–chromium distance is 2.327 Å (B3LYP) or 2.267 Å (BP86), which is shorter by 0.074 Å than that for $(\text{OC})_3\text{MnMn}(\text{CO})_5$.

3.2. Vibrational Frequencies. The first three low-lying structures can be considered as minima on the potential energy surface (PES), with the small observed imaginary harmonic vibrational frequencies being an artifact of the DFT method. An interesting contradiction again exists between the B3LYP and BP86 functionals for the global minimum structure of $\text{Cr}_2(\text{CO})_8$ (Figure 1) as in the previous work on $\text{Cr}_2(\text{CO})_9$.⁸ Only the BP86 method predicts one small imaginary frequency 28 cm^{-1} (a'') for the lowest-energy structure, and it is predicted to be a genuine minimum with the B3LYP method. For other isomers, the two methods agree with each other very well.

The B3LYP and BP86 vibrational frequencies for the five isomers of $\text{Cr}_2(\text{CO})_8$ are listed in Tables 2–6 (Supporting Information). As expected, the CO stretching frequencies have the highest infrared intensities and are expected to dominate the vibrational spectrum. Note also that, for molecules such as $\text{Mn}_2(\text{CO})_{10}$, $\text{Fe}_2(\text{CO})_9$, and $\text{Co}_2(\text{CO})_8$, the BP86 method predicts vibrational frequencies more reliably than B3LYP. For $\text{Mn}_2(\text{CO})_{10}$, for example, the agreement between BP86 and experimental CO stretching frequencies is typically within 10 cm^{-1} .

3.3. Thermochemistry. The energy of unsymmetrical dissociation of $\text{Cr}_2(\text{CO})_8$ to $\text{Cr}(\text{CO})_3$ and $\text{Cr}(\text{CO})_5$ fragments is predicted to be 35 kcal/mol with the B3LYP functional or 44 kcal/mol with the BP86 functional. Similarly, the energy of symmetrical dissociation of $\text{Cr}_2(\text{CO})_8$ to two $\text{Cr}(\text{CO})_4$ fragments

is computed to be 34 kcal/mol (B3LYP) or 44 kcal/mol (BP86). This demonstrates that the interaction between the two chromium fragments for $\text{Cr}_2(\text{CO})_8$ is similar to that previously found for $\text{Cr}_2(\text{CO})_9$, but different from the much weaker interactions between the two mononuclear chromium carbonyl fragments found for $\text{Cr}_2(\text{CO})_{10}$ and $\text{Cr}_2(\text{CO})_{11}$. For comparison, the dissociation energy of $\text{Cr}_2(\text{CO})_9$ to $\text{Cr}(\text{CO})_4$ and $\text{Cr}(\text{CO})_5$ fragments is predicted to be 32 kcal/mol with the B3LYP functional or 43 kcal/mol with the BP86 functional, whereas dissociation to $\text{Cr}(\text{CO})_3$ and $\text{Cr}(\text{CO})_6$ fragments is predicted to be 41 kcal/mol (B3LYP) or 30 kcal/mol (BP86). The dissociation energy of $\text{Cr}_2(\text{CO})_9$ to $\text{Cr}_2(\text{CO})_8$ and CO is calculated to be 37 kcal/mol with the B3LYP functional or 44 kcal/mol with the BP86 functional.

3.4. Molecular Orbitals. Electron density plots of the six valence molecular orbitals (MOs) of $\text{Cr}_2(\text{CO})_8$ in C_s symmetry are shown in Figure 6. These range from the sixth highest occupied orbital (HOMO-5) to the highest occupied orbital (HOMO). The symmetry-adapted linear combinations of the d atomic orbitals provide the bonding and antibonding interactions between the metal atoms. The results suggest that HOMO-5, HOMO-4, and HOMO-3 are primarily the direct d–d bonding orbitals. For instance, HOMO-5 appears to be a strong Cr–Cr σ -bonding orbital. The orbitals with antibonding character appear to be HOMO-2, HOMO-1, and HOMO.

Comparison plots have been made for the $\text{Cr}_2(\text{CO})_9$ molecule, global minimum of C_s symmetry, and these are seen in Figure 7. Basically, the MOs of the $\text{Cr}_2(\text{CO})_9$ are rather similar to those of $\text{Cr}_2(\text{CO})_8$. The similarity of the MOs suggests that $\text{Cr}_2(\text{CO})_8$ is a potentially stable molecule like $\text{Cr}_2(\text{CO})_9$. It also explains the similarity of the dissociation energies to fragments from $\text{Cr}_2(\text{CO})_8$ and $\text{Cr}_2(\text{CO})_9$.

4. Concluding Remarks

The $\text{Cr}_2(\text{CO})_5(\mu\text{-CO})_3$ global minimum for $\text{Cr}_2(\text{CO})_8$ (Figure 1) is closely related to the $\text{Cr}_2(\text{CO})_6(\mu\text{-CO})_3$ global minimum predicted for $\text{Cr}_2(\text{CO})_9$ by removal of one of the terminal CO groups. The chromium–chromium distance for this isomer of $\text{Cr}_2(\text{CO})_8$ is 2.29 ± 0.01 Å, which is only ~ 0.02 Å shorter than

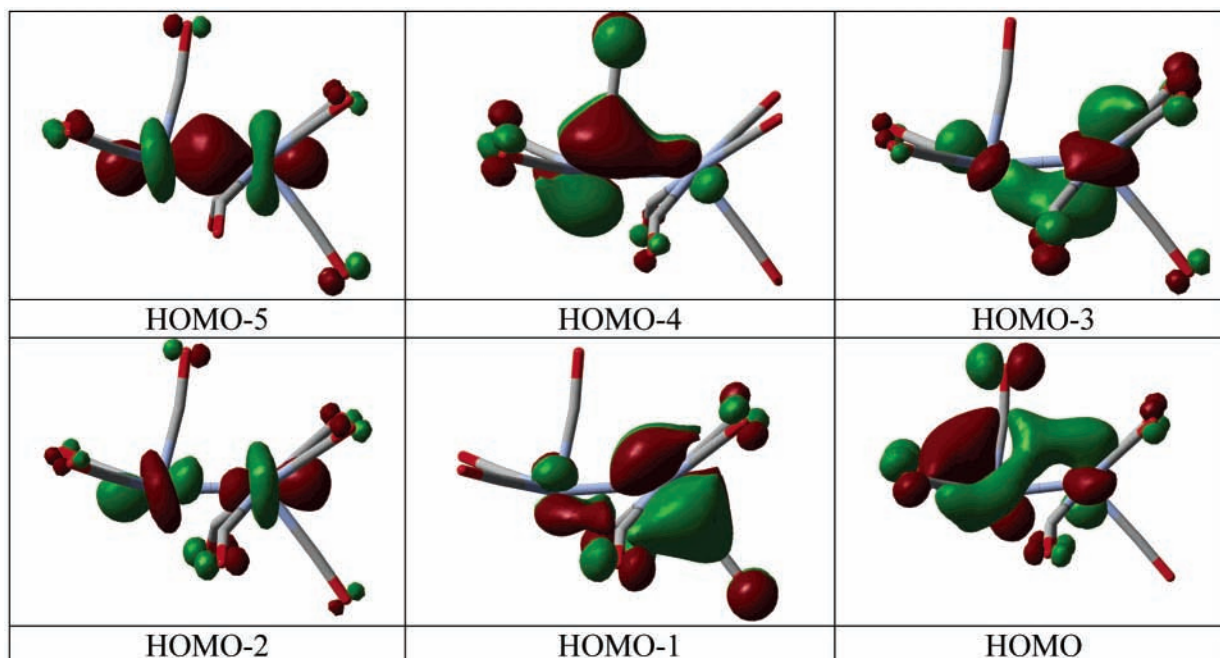


Figure 6. Valence molecular orbital plots for singlet $\text{Cr}_2(\text{CO})_8$ in C_2 symmetry, showing from the sixth highest occupied valence molecular orbital HOMO-5 up to the HOMO.

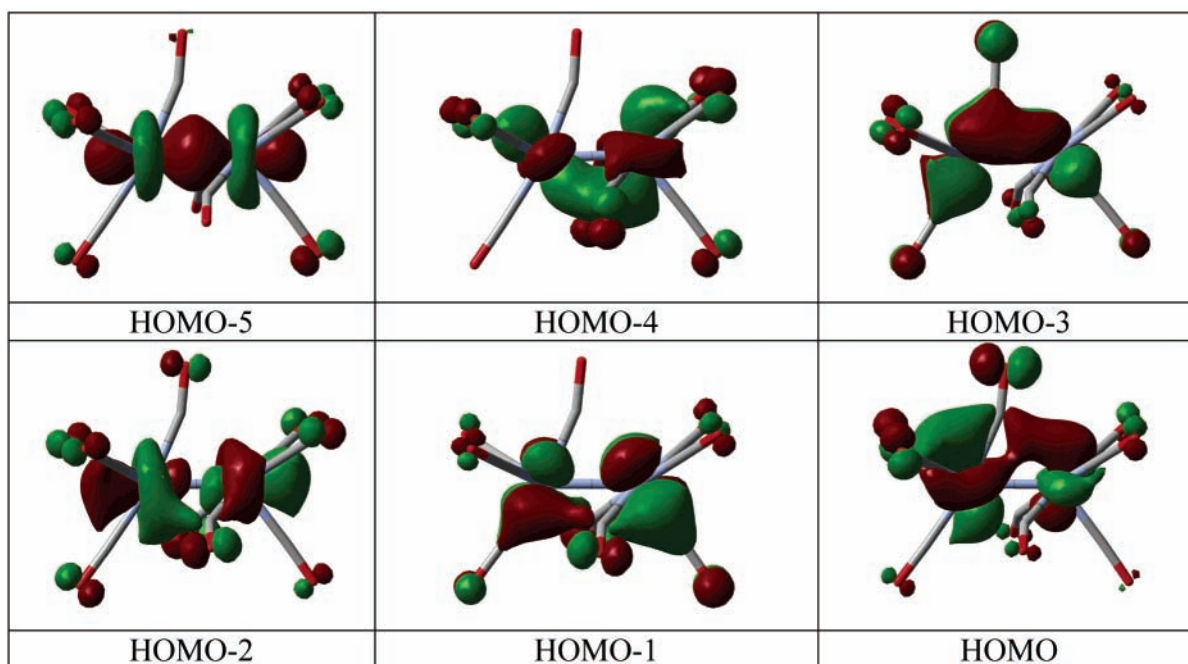


Figure 7. Valence molecular orbital plots for singlet $\text{Cr}_2(\text{CO})_9$ in C_2 symmetry, showing from the sixth highest occupied valence molecular orbital HOMO-5 up to the HOMO.

the chromium–chromium distance of $2.30 \pm 0.02 \text{ \AA}$ obtained for the global minimum of $\text{Cr}_2(\text{CO})_9$. This suggests that, in $\text{Cr}_2(\text{CO})_8$, the formal chromium–chromium bond order remains three, but only one of the two Cr atoms goes from an 18-electron to a 16-electron configuration by losing a CO group.

The next two higher-lying structures computed for $\text{Cr}_2(\text{CO})_8$ (Figures 2 and 3) both are $\text{Cr}_2(\text{CO})_6(\mu\text{-CO})_2$ structures with two bridging CO groups so oriented to be four-electron donors, using the π -orbitals of the CO multiple bond as well as the carbon lone pair. A $\text{Cr}=\text{Cr}$ formal double bond is then sufficient to give each chromium atom the favored 18-electron rare gas configuration. In the more symmetrical structure (Figure 2), the two bridging CO groups connect two $\text{Cr}(\text{CO})_3$ units, and the

$\text{Cr}=\text{Cr}$ distance is 2.49 \AA . In the less symmetrical structure (Figure 3), the two bridging CO groups link a $\text{Cr}(\text{CO})_4$ unit and a $\text{Cr}(\text{CO})_2$ unit. The chromium–chromium distance is significantly longer ($2.73 \pm 0.02 \text{ \AA}$) in this isomer but still short enough to be considered as a $\text{Cr}=\text{Cr}$ formal double bond (the anticipated $\text{Cr}-\text{Cr}$ single bond distance is around 3.0 \AA).

Although the two highest-lying isomers considered for $\text{Cr}_2(\text{CO})_8$ (Figures 4 and 5) are nonbridged structures, symmetrical or unsymmetrical, the chromium–chromium distances are not shortened significantly, in the range of the formal triple bond distance $2.2\text{--}2.3 \text{ \AA}$.

The following two conclusions may be drawn from this DFT study on $\text{Cr}_2(\text{CO})_8$:

(1) The chromium–chromium distance in none of the Cr₂(CO)₈ isomers is short enough to suggest unambiguously a formal chromium–chromium quadruple bond. Thus, the shortest chromium–chromium distance found for any of isomers is ~2.2 Å, which is appreciably longer than most of the known chromium–chromium distances (typically 1.8–2.0 Å) in chromium(II) derivatives formulated with chromium–chromium quadruple bonds. The global minimum Cr₂(CO)₅(μ-CO)₃ structure for Cr₂(CO)₈ (Figure 1) avoids a formal chromium–chromium quadruple bond by having an unsaturated 16-electron configuration rather than a saturated 18-electron configuration for one of the chromium atoms. The next two higher-energy structures for Cr₂(CO)₈ are of the Cr₂(CO)₆(μ-CO)₂ type and avoid a formal chromium–chromium quadruple bond by having two four-electron donor bridging carbonyl groups. The two highest-energy unbridged structures for Cr₂(CO)₈ have longer formal (not actual) chromium–chromium quadruple bonds by adopting the unfavorable staggered or unsymmetrical structure configurations. The different formal metal oxidation states and the different types of ligands may account for the appreciably longer chromium–chromium distances.

(2) The thermodynamics indicates that Cr₂(CO)₈, like Cr₂(CO)₉, is stable with respect to dissociation into mononuclear fragments. It thus might be a reasonable synthetic objective. However, a feasible synthetic route would need to avoid the Cr₂(CO)₁₁ or Cr₂(CO)₁₀ intermediates since these latter binuclear derivatives are thermodynamically unstable with respect to mononuclear species. This, as well as the high unsaturation of Cr₂(CO)₈, imposes severe constraints for the synthesis of Cr₂(CO)₈ and might account for the fact that it has not yet been synthesized.

Acknowledgment. We are grateful for the support of this work by NSF Grants CHE-0136186 and CHE-0209857.

Supporting Information Available: Tables 2–6 list B3LYP and BP86 harmonic vibrational frequencies (cm⁻¹) and their infrared intensities (km/mol) for the five isomers of Cr₂(CO)₈. This material is available free of charge via the Internet at <http://pubs.acs.org>.

References and Notes

- (1) Kenny, J.; King, R. B.; Schaefer, H. F. *Inorg. Chem.* **2001**, *40*, 900.
- (2) Xie, Y.; King, R. B.; Schaefer, H. F. *J. Am. Chem. Soc.* **2000**, *122*, 8746.
- (3) Xie, Y.; Jang, J. H.; King, R. B.; Schaefer, H. F. *Inorg. Chem.* **2003**, *42*, 5219.
- (4) Green, M. L. H. *J. Organomet. Chem.* **1995**, *500*, 127.
- (5) The required monograph on metal–metal multiple bonds is Cotton, F. A.; Walton, R. A. *Multiple Bonds between Metal Atoms*, 2nd ed.; Clarendon Press: Oxford, U.K., 1993.
- (6) Richardson, N. A.; Xie, Y.; King, R. B.; Schaefer, H. F. *J. Phys. Chem. A* **2001**, *105*, 11134.
- (7) Li, S.; Richardson, N. A.; Xie, Y.; King, R. B.; Schaefer, H. F. *Faraday Discuss.* **2003**, *124*, 315.
- (8) Li, S.; Richardson, N. A.; King, R. B.; Schaefer, H. F. *J. Phys. Chem. A* **2003**, *107*, 10118.
- (9) Cotton, F. A.; DeBoer, B. G.; LaPrade, M. D.; Pipal, J. R.; Ucko, D. A. *J. Am. Chem. Soc.* **1970**, *92*, 2926.
- (10) Krause, J.; Marx, G.; Schodl, G. *J. Organomet. Chem.* **1970**, *21*, 159.
- (11) Aoki, T.; Furusaki, A.; Tomiie, Y.; Ono, K.; Tanaka, K. *Bull. Chem. Soc. Jpn.* **1969**, *42*, 545.
- (12) Cotton, F. A.; Koch, S.; Millar, M. *J. Am. Chem. Soc.* **1977**, *99*, 7372.
- (13) Cotton, F. A.; Koch, S. A.; Millar, M. *Inorg. Chem.* **1978**, *17*, 2087.
- (14) Dunning, T. H. *J. Chem. Phys.* **1970**, *53*, 2823.
- (15) Huzinaga, S. *J. Chem. Phys.* **1965**, *42*, 1293.
- (16) Wachters, A. J. H. *J. Chem. Phys.* **1970**, *52*, 1033.
- (17) Hood, D. M.; Pitzer, R. M.; Schaefer, H. F. *J. Chem. Phys.* **1979**, *71*, 705.
- (18) Ziegler, T. *Can. J. Chem.* **1995**, *73*, 743.
- (19) Becke, A. D. *J. Chem. Phys.* **1993**, *98*, 5648.
- (20) Lee, C.; Yang, W.; Parr, R. G. *Phys. Rev. B* **1988**, *37*, 785.
- (21) Jonas, V.; Thiel, W. *Organometallics* **1998**, *17*, 353.
- (22) Becke, A. D. *Phys. Rev. A* **1988**, *38*, 3098.
- (23) Perdew, J. P. *Phys. Rev. B* **1986**, *33*, 8822; *34*, 7046.
- (24) Frisch, M. J.; Trucks, G. W.; Schlegel, H. B.; Gill, P. M. W.; Johnson, B. G.; Robb, M. A.; Cheeseman, J. R.; Keith, T. A.; Petersson, G. A.; Montgomery, J. A.; Raghavachari, K.; Al-Laham, M. A.; Zakrzewski, V. G.; Ortiz, J. V.; Foresman, J. B.; Cioslowski, J.; Stefanov, B. B.; Nanayakkara, A.; Challacombe, M.; Peng, C. Y.; Ayala, P. Y.; Chen, W.; Wong, M. W.; Andres, J. L.; Replogle, E. S.; Gomperts, R.; Martin, R. L.; Fox, D. J.; Binkley, J. S.; Defrees, J. D.; Baker, J.; Stewart, J. P.; Head-Gordon, M.; Gonzalez, C.; Pople, J. A. *Gaussian 94*, revision B.3; Gaussian, Inc: Pittsburgh PA, 1995.
- (25) Barckholtz, T. A.; Bursten, B. E. *J. Am. Chem. Soc.* **1998**, *120*, 1926.